Methionine restriction improves renal insulin signalling in aged kidneys

Louise Grant [a], Emma K. Lees[a], Laura A. Forney[b], Nimesh Mody[a], Thomas Gettys[b], Paul AJ. Brown[c], Heather M. Wilson[a], Mirela Delibegovic[a].

Author Affiliations:

a. Institute of Medical Sciences, University of Aberdeen, College of Life Sciences and Medicine, Foresterhill Health Campus, Aberdeen, UK.
b. Nutrient Sensing and Adipocyte Signaling Department, Pennington Biomedical Research Center, Baton Rouge, LA 70808, USA.
c. Pathology Department, Aberdeen Royal Infirmary, Aberdeen, UK.

Corresponding authors: Mirela Delibegovic, m.delibegovic@abdn.ac.uk and Heather Wilson, h.m.wilson@abdn.ac.uk

Abstract

Dietary methionine restriction (MR) leads to loss of adiposity, improved insulin sensitivity and lifespan extension. The possibility that dietary MR can protect the kidney from age-associated deterioration has not been addressed. Aged (10-month old) male and female mice were placed on a MR (0.172% methionine) or control diet (0.86% methionine) for 8-weeks and blood glucose, renal insulin signalling, and gene expression were assessed. Methionine restriction lead to decreased blood glucose levels compared to control-fed mice, and enhanced insulin-stimulated phosphorylation of PKB/Akt and S6 in kidneys, indicative of improved glucose homeostasis. Increased expression of lipogenic genes and downregulation of *PEPCK* were observed, suggesting that kidneys from MR-fed animals are more insulin sensitive. Interestingly, renal gene expression of the mitochondrial uncoupling protein *UCP1* was upregulated in MR-fed animals, as were the anti-ageing and renoprotective genes *Sirt1*, *FGF21*, *klotho*, and *β-klotho*. This was associated with alterations in renal histology trending towards reduced frequency of proximal tubule intersections containing vacuoles in mice that had been on dietary MR for 190 days compared to control-fed mice, which exhibited a pre-diabetic status. Our results indicate that dietary MR may offer potential in ameliorating the renal functional decline related to ageing and other disorders associated with metabolic dysfunction by enhancing renal insulin sensitivity and renoprotective gene expression.

Keywords

Methionine, Diet, Kidney, Ageing, Insulin, Renoprotection

1. Introduction

The accumulation of visceral fat is associated with ageing and is strongly linked to the development of metabolic disorders including insulin resistance (1, 2). Surgical removal of visceral fat or reduction in adiposity by caloric restriction (CR), are effective strategies in rodents for increasing lifespan and enhancing insulin sensitivity (2-4). Reducing dietary levels of the essential amino acid methionine also extends lifespan (5, 6). The advantage of dietary MR is that its benefits do not require restriction of food intake.

Our group has recently demonstrated that a MR diet can reverse age-induced metabolic dysfunction in adult mice by lipid homeostasis remodelling in the liver and white adipose tissue (WAT), and enhance insulin sensitivity in peripheral tissues (7). The occurrence of age-related glucose intolerance due to defective insulin secretion, clearance and peripheral tissue responses to insulin, is also well documented (8). Kidney function is also known to significantly decline with age with an estimated average loss of glomerular filtration rate (GFR) of approximately 1 millilitre per year and an increased predisposition to glomerulosclerosis and interstitial fibrosis (9, 10).

To our knowledge, no studies have investigated the effects of MR on kidney insulin sensitivity and we hypothesised that MR dietary intervention may be a viable measure for protecting against renal dysfunction as a consequence of age-related glucose intolerance by improving renal insulin signalling. To provide proof-of-principle data for further human intervention studies, we used aged mice to test this hypothesis.

2. Materials and Methods

2.1 Animal studies.

All animal procedures were approved by the University of Aberdeen Ethics Review Board and performed under UK Home Office project license PPL60/3951 and according to the ARRIVE guidelines. Ten-month old male and female C57BL/6J wild-type mice (Charles River, Edinburgh, UK) were singly housed and maintained at 22-24ºC on 12-hour light/dark cycle with free access to food/water. Mice were maintained on a control diet (0.86% methionine) (Dyets, Bethlehem, PA, USA) for two weeks. They were then randomised into two groups based on body weight with one group given control diet and the other given MR diet containing 0.172% methionine (Dyets, Bethlehem, PA, USA), as described previously (7). The mice were maintained on each diet for 8 weeks and terminal tissues harvested after 5 hour fasting. For insulin signalling experiments, male mice only were investigated. Intraperitoneal *(i.p.)* injection with saline (154 mM NaCl) or insulin (10 mU/g body weight) was administered after 5 hour fast, and mice sacrificed by cervical dislocation after 10 min. Kidneys were harvested and frozen immediately in liquid nitrogen. For histological analysis, 8-week old male C57BL/6J wild-type mice were randomised to MR or control dietbased on body weight, for 190 days before kidneys were harvested and fixed in ethanol and stored at 4°C before wax embedding and sectioning. Body composition for long-term experiment was measured by NMR using a Bruker Minispec (Billerica, MA).

2.2 Blood metabolites and whole body measurements.

Tail vein blood samples were obtained after a 5 hour fast and blood glucose measurements taken using glucometers (AlphaTRAK, Berkshire, UK), 6 weeks after the initiation of the diets. For the long-term MR diet study, tail vein blood samples were obtained after a 5 hour fast and serum insulin levels were measured by ELISA as per the manufacturer's instructions (EMD Millipore,Temecula, CA).

2.3 Immunoblotting

Frozen kidney lysates were prepared in radioimmunoprecipitation-assay (RIPA) buffer containing fresh sodium-orthovanadate and protease-inhibitors (11). Proteins were separated by 4-12% SDS-PAGE and transferred to nitrocellulose membranes. Immunoblots were performed using antibodies from Cell Signaling *(*NEB, Hitchin, UK) (unless stated otherwise) against phospho-Akt/PKB (s473), total Akt/PKB A2210 (Santa Cruz, Dallas, TX, USA), phospho-S6 ribosomal protein (s235/236), total S6 2217S, phospho-IR (tyr1162/1163) 44804G (Invitrogen, Paisley, UK), phospho-IR (tyr1158), IR-βsc-

711 (Santa-Cruz, Dallas, TX, USA), β-actin (Thermo Scientific, Waltham, USA), cytochrome C, mitochondrial transcription factor (TFAM), PGC1α (Abcam, Cambridge, UK), UCP1 (Abcam, Cambridge, UK) . Immunoblots were visualized using enhanced-chemiluminescence, and quantified by densitometry scanning using Bio1D-software *(*PeqLab, Fareham, UK*)*.

2.4 Gene-expression analysis.

Frozen kidney sections were homogenized in TriFast reagent (Peqlab, UK) (20). cDNA synthesis was carried out from 1 µg of RNA using Tetro cDNA-synthesis kit (Bioline, London, UK). Target genes were amplified by quantitative real-time PCR using gene-specific primers (Sigma, UK) and GoTaq master mix (Promega, Southampton, UK) using the Light-Cycler 480 (Roche). Relative mRNA levels were calculated using the Pfaffl method (12) and normalised to the most stable reference gene (YWhaz, NoNo, GAPDH, HPRT or β-actin) which was identified using a web-based reference gene assessment tool *(*http://www.leonxie.com/referencegene.php?type=reference). Primer sequences are provided in supplementary material.

2.5 Histological analysis

Kidney tissue was fixed in formaldehyde, embedded in paraffin, sectioned at 5µm, and stained with haematoxylin and eosin. Slides were scored using a graticule at x20 magnification by Dr Paul AJ Brown, consultant pathologist, Aberdeen Royal Infirmary, who was blinded to the study. 100 random intersections were examined for each kidney and a score of 0 or 1 was given for each tubular profile involving an intersection: 0 = normal histology; 1 = vacuole(s) involving that tubular profile. The total score for each kidney was calculated by addition of all 100 scores with a maximum score of 100.

2.6 Statistical analysis.

Data are expressed as mean ± SEM. Statistical analyses were performed using one-way ANOVA with Tukey's multiple comparison post-tests, two-way ANOVA with Bonferroni-multiple comparisons post-tests, and two-tailed Student's t-tests, as appropriate, using GraphPad Prism 5 statistical-software (GraphPad Sortware Inc., San Diego, CA, USA). *P*-values < 0.05 were considered significant.

3. Results

3.1 MR diet decreases fasting glucose levels, improves glucose tolerance and enhances renal insulin signalling

Eight weeks of dietary MR produced significant decreases in fasting blood glucose levels in both male and female mice when compared to control littermates (*fig. 1A*). Glucose tolerance testing (GTT) revealed an improvement in glucose tolerance in MR-diet fed male mice compared to controls *(fig 1B)*, in both males and females, as represented by Area Under the Curve (AUC). To test the impact of dietary MR on insulin signalling in the kidney, renal tissue (medulla and cortex) was harvested from male mice after a 5 h fast and acute injection with insulin (10mU/g body weight) (*fig 1C*). Following insulin binding, a number of tyrosine residues including tyrosines 1158, 1162, and 1163 on the insulin receptor (IR) become autophosphorylated, leading to the phosphorylation of target substrates including IRS proteins (13). The phosphorylation of PKB/Akt also activates mTORC1 leading to increased protein synthesis, via activation of S6K1 and its target S6 (14) Diet-induced increases in insulin-dependent PKB/Akt and S6 phosphorylation were observed with no effect on insulin activation of its receptor, suggesting that MR amplifies insulin signal downstream of IR, at the level of PKB/Akt (*fig 1C and 1D*). The enhancement of insulin-induced phosphorylation of PKB/Akt and S6 by dietary MR, in conjunction with diet-induced reductions in fasting glucose, are consistent with both global and tissue-specific effects of dietary MR on insulin sensitivity.

3.2 MR diet increases lipogenic gene expression in the kidney

In view of the improved glucose homeostasis and enhanced diet-dependent insulin signalling observed in the MR-diet mice, we investigated diet-dependent effects on lipid metabolism in the kidney, where it was hypothesised that a more insulin sensitive state would be reflected in increased lipogenesis and inhibition of gluconeogenesis.

Insulin promotes *de novo* lipogenesis (DNL) by activating the lipogenic transcription factor *sterol regulatory element-binding protein 1c (SREBP1c).* For example, *acetyl-CoA carboxylase (ACC)* and *fatty acid synthase (FAS)* regulate key steps in fatty acid biosynthesis and both are regulated by *SREBP1c* (15). Most notably in females, dietary MR increased renal expression of *FAS*, *SREBP1c*, and the *ACC1 and ACC2* isoforms of *ACC* (*fig 2A*). A similar pattern was found in the MR-fed male mice, but only the increase in *ACC2* expression reached significance, in addition to another promoter of lipogenesis, *peroxisome proliferator-activated-receptor gamma (PPARγ)* (*fig 2B*). Dietary MR in female mice led to suppressed expression of the gluconeogenic gene, *phosphoenolpyruvate carboxykinase* (*PEPCK*) in kidneys compared to controls (*fig 2A*).

3.3 MR diet upregulates *UCP1* and renoprotective gene expression

Methionine restriction significantly upregulated renal expression of *fibroblast growth factor* (*FGF21)*, *Klotho* and *β-Klotho* mRNA in females, and *Sirtuin 1* (*Sirt1)* mRNA expression in male kidneys (*fig 3A and 3B*); all of which possess renoprotective properties (16-18).

Dietary MR was previously shown to increase expression of adipose uncoupling protein-1 *(UCP1)* (19). To our knowledge, little is known about the function or even the expression of *uncoupling protein 1 (UCP1)* in mouse kidney. In this study we observed abundant expression of renal *UCP1* which was significantly elevated in the female MR group compared to control. Protein levels of UCP1, however, were variable between subjects and no significant differences were observed between treatment groups in females and males (*fig A and B, respectively*). This was also the case for other proteins involved in mitochondrial biogenesis (proliferator-activated receptor γ coactivator 1; PGC1α, transcription factor A, TFAM, and cytochrome C) (*fig A and 4B).*

3.4 Renal pro-inflammatory gene expression is not upregulated by MR diet

The presence of chronic low-grade inflammation is a hallmark of numerous age-related conditions including the decline in renal function that is observed with increasing age (20, 21). It was therefore of interest to determine gene expression levels of a panel of pro-inflammatory and anti-inflammatory markers in aged kidneys from mice fed MR and control diet. Renal expression of the pro-inflammatory mediators *tumour necrosis factor-alpha (TNFα*), interleukin-6 (IL-6), interleukin-1-beta (IL-1β), and *monocyte chemoattractant protein-1 (MCP-1)* and markers of macrophage accumulation the macrophage *F4/80 receptor (F4/80), cluster of differentiation molecule-11b (CD11b),* and *cluster of differentiation molecule-68 (CD68)* in female and male MR groups were unchanged when compared to control mice (*fig 5A and 5B*, respectively). The pro-fibrotic mediators, *platelet derived growth factor-B (PDGF-B)* and *transforming growth factor-beta (TGF-β)* were also unaltered by MR diet. (*fig 5A*).

3.5 Long-term MR diet decreases body weight, fat mass and serum insulin levels

As expected, long-term (190 day) MR diet significantly decreased body weight (as measured in the final 3 weeks of the study) compared to control diet *(fig 6A)*. A significant decrease in lean mass (g) was observed in MR-fed mice *(fig 6B)* but when calculated as a percentage of total body weight, lean mass was found to be significantly increased by MR diet compared to control diet (*fig 6C*). Methionine restriction significantly decreased total body fat (*fig 6D*) and percentage body fat (*fig 6E*) compared to control diet fed mice. Fasting insulin levels were also found to be significantly decreased by long-term MR feeding *(fig 6F)*.

3.6 Long-term MR diet offers some protection against renal damage

With increasing age, the kidney is less effective at concentrating or diluting urine and more likely to retain salt, and these dysfunctions are associated with age-associated histological changes (8). In order to investigate the effect of MR diet on the ageing kidney, renal histology was assessed in mice which had been fed the MR or control diet for a prolonged period of 190 days. It was observed that there was an non-significant increase in vacuoles within the proximal convoluted tubules in control aged kidneys, whilst MR-fed kidneys offered a degree of protection, as determined by H and E staining (*fig 7 A, B, C*). This did not appear to correlate to body weight or serum insulin levels measured in these mice ((*fig 7 D, E*).

4. Discussion

Dietary MR offers promise as an intervention for the treatment of metabolic dysfunction due to its ability to reduce body weight and adiposity, despite an increase in food intake (5, 19). Moreover, dietary MR improves insulin sensitivity and glucose/lipid homeostasis in rodents and humans (7, 19, 22, 23). Kidney function is known to decline with age and is exacerbated by an age-related occurrence of increased insulin resistance, inflammation, and oxidative stress (8). With regard to dietary modifications, caloric restriction (CR) has proven to be the most efficacious mode of protecting against the onset of age-related kidney damage in rodent models (24). In this study we sought to elucidate the effect of dietary MR, which unlike CR permits *ad libitum* feeding, on whole body glucose homeostasis, renal insulin signalling, lipogenic and inflammatory gene expression, and histology in aged mice.

Following 8 weeks on MR diet, mice had significantly improved glucose tolerance, and lower fasting blood glucose levels than controls indicative of improved glucose homeostasis, as reported previously (7). In addition, levels of insulin-stimulated phosphorylated proteins within the insulin signalling cascade (PKB/Akt and S6) were significantly greater in kidneys of mice fed a MR diet compared to controls. The tissue-specific enhancement of insulin signalling by MR is in agreement with similar studies looking at white adipose tissue (WAT), liver and muscle and reinforces the potential application of MR diet as a protective dietary intervention against age-associated metabolic dysfunction (7). Interestingly, a recent paper demonstrated that very low protein diet ameliorates advanced diabetic nephropathy (35), associated with suppression of p-S6 ribosomal protein (p-S6RP), which is in line with the data presented in this manuscript. We also observed upregulation of genes involved in lipogenesis and suppressed expression of the gluconeogenic gene, *PEPCK* in the kidney of MR mice compared to controls inferring improved insulin responsiveness. A similar upregulation in lipogenic genes has been observed in white adipose tissue from MR diet-fed mice with a concomitant decrease in hepatic lipogenic gene expression, and it is believed that this metabolic remodelling may lead to improved insulin sensitivity (7, 25).

It has been postulated that the loss of adiposity despite increased consumption of a MR diet is due, at least in part, to elevated energy expenditure driven by UCP-1 nonshivering thermogenesis in adipose tissue (19) and MR has recently been shown to greatly upregulate UCP-1 expressing cells in inguinal WAT leading to increased respiratory capacity (26). However, the function of UCP1 in the kidney is not known. Conflicting reports have been published on the presence of UCP-1 in the rodent kidney (27, 28), however our data clearly shows that *UCP-1* is highly expressed at the *mRNA* level and, albeit with high variability between replicates, at the protein level too. We observed substantial upregulation, most notably in the females, of renal *UCP-1* gene expression in MR mice compared to controls. Although at the protein level, a MR diet was found to exert no effect on levels of UCP-1 and other mitochondrial biogenesis markers, the significant increase in renal *UCP-1* gene expression is of interest and worthy

of future investigation. The notable sexual dimorphism apparent for the gene expression profiles, whereby female mice exhibited greater dietary-induced changes than males, is also of significance. Substantial evidence exists to suggest that male kidneys are more vulnerable to age-related decline in renal function than females (20, 24, 29, 30).

Our group has recently demonstrated that short-term MR treatment (48 hr) is sufficient to significantly increase circulating levels and hepatic expression of FGF21 in mice (7). This was associated with improvements in insulin sensitivity, independent of changes in body composition or weight. Similarly, in this study we observed an upregulation of renal *FGF21* mRNA in MR-fed mice compared to controls which may contribute to the insulin-sensitizing effects observed in the kidneys of these animals. FGF21 is a hormone released by the liver in response to caloric restriction and markedly extends the lifespan of mice when overexpressed (31). The kidney has been identified as a target of FGF21, and exogenous administration of FGF21 protein has been shown to improve systemic metabolism and exert anti-fibrotic properties in kidneys of *db/db* mice (16). More recently, it has been demonstrated that upregulation of renal *FGF21* expression in streptozotocin-treated C57/BL mice leads to a significant renal protection, believed to be due to PI3K/Akt/GSK3β/Fyn-mediated activation of the Nrf2 anti-oxidative pathway (32). In this study we identified significant upregulation of renal *FGF21 mRNA* in MR-fed females, in addition to increased expression of the FGF21 co-receptor, *β-Klotho*. *Klotho* which is highly expressed in the kidney, was also significantly upregulated by a MR diet and has been deemed of therapeutic interest due to the observation that klotho deficiency is associated with increased susceptibility to injury and fibrosis with prolonged kidney recovery (33). Sirt-1, which also exerts renoprotective effects and regulates lipid and glucose metabolism, has been identified as another therapeutic target for renal diseases (18), and was found to be elevated at the *mRNA* level in kidneys from MR-fed male mice. Taken together, these gene expression alterations associated with the adoption of dietary MR, may reduce the decline in renal function that is associated with ageing.

Chronic low-grade inflammation is known to play a role in the degenerative processes associated with the ageing kidney (20, 21). In this study, renal gene expression of pro-inflammatory cytokines or pro-fibrotic mediators were reassuringly unaltered by MR diet. Interestingly, levels of anti-inflammatory genes IL-10 and IL-4, showed the biggest increase in kidneys from MR diet-fed animals compared to control suggesting a potential protective effect by MR. Histological evidence of chronic renal damage was not observed in these animals, but there was evidence of tubular injury. There was a trend towards increased presence of proximal tubule vacuoles in control aged kidneys compared to those from mice on long-term MR diet, which was not due to decreased body weight/adiposity or serum insulin (34). The underlying cause of this histological damage is uncertain and requires further study.

These data suggest that dietary manipulation by MR in mice enhances renal insulin signalling and increases expression of genes involved in lipogenesis, thermogenesis and renoprotection without

affecting levels of pro-inflammatory mediators in aged mice. Since the ageing kidney can display a number of non-specific changes that have similarities to those observed in diabetic nephropathy (DN), positive findings may be of therapeutic value to this condition too. It would be of merit to use mouse models of DN to assess whether MR dietary intervention is able to delay, prevent or reverse the fibrotic and pro-inflammatory phenotype observed in these models. Positive findings may translate into a new therapeutic dietary intervention for DN and other disorders associated with metabolic dysfunction.

Figure legends

Figure 1. Blood glucose levels, glucose tolerance and renal insulin signalling of mice on a methionine restriction (MR) and control diet. (A) Mice fed a MR-diet (n = 10 for males and n = 7 for females) for

8 weeks had significantly lower blood glucose levels than their control diet counterparts (n = 9 for males and n = 7 for females). Significance was calculated by 2–tailed Student's *t*-test. Data are represented as mean ± SEM. White bars represent control-fed mice and black bars represent MR-fed mice. (B) Glucose tolerance testing (2g/kg glucose dose) was carried out after 6 weeks on diets after a 5-h fast in male mice and female mice and data was expressed as area under the curve. Significance was calculated by r 2-tailed Student's *t*-tests. (C) Insulin signalling was measured by administering saline (n = 3) or insulin (10 mU/g of body weight; n = 5) to male mice *i.p*. after a 5-h fast (*P<0.05). Mice were sacrificed 10 min after injection and tissues harvested for analysis. Levels of phosphorylated IR (tyr1162/1163 and tyr1158), Akt (ser473), S6 (ser235/236), IR-β, total Akt, total S6, and β-actin were determined by immunoblotting (C) and normalised to total proteins. (D) Data were analysed as fold change relative to control-fed insulin-injected mice. Significance was calculated by two-tailed Student's *t*-test (*P<0.05) (D). Data are represented as mean ± SEM. Checked bars represent control (saline) mice, white bars represent control (insulin) mice, striped bars represent MR (saline) mice, and black bars represent MR (insulin) mice.

Figure 2. Renal expression of genes pertinent to lipid and glucose metabolism in mice fed control or methionine restriction (MR) diet for 8 weeks in (A) female mice (n = 6 – 8) and (B) male mice (n = 7 – 10) as determined by qPCR. Data were analysed as fold change relative to control-fed mice. Significance was calculated by two-tailed Student's t-test (*P<0.05). Data are represented as mean ± SEM. White bars represent control-fed mice and black bars represent MR-fed mice.

Figure 3. Renal expression of genes pertinent to mitochondrial biogenesis and renoprotection in mice fed control or methionine restriction (MR) diet for 8 weeks in (A) female mice (n = 6 – 8) and (B) male mice (n = 7 – 10) as determined by qPCR. Data were analysed as fold change relative to control-fed mice. Significance was calculated by two-tailed Student's t-test (*P<0.05). Data are represented as mean ± SEM. White bars represent control-fed mice and black bars represent MR-fed mice.

Figure 4. Levels of mitochondrial biogenesis markers present in kidneys from mice fed control or methionine restriction (MR) diet for 8 weeks. Protein levels of PGC1α, UCP1, TFAM and cytochrome C were determined by immunoblotting for (A) female, and (B) male mice, and normalised to β-actin. Data were analysed as fold change relative to control mice. Significance was calculated by two-tailed Student's t-test (*P<0.05). Data are represented as mean ± SEM. White bars represent control-fed mice and black bars represent MR-fed mice.

Figure 5. Pro-inflammatory and anti-inflammatory gene expression in kidneys from mice fed control or methionine restriction (MR) diet for 8 weeks. Gene expression was measured by qPCR in kidneys from (A) female mice (n = 6 – 8) and (B) male mice (n = 7 – 10) fed control or MR diet. Data were analysed as fold change relative to control-fed mice. Significance was calculated by two-tailed Student's t-test (*P<0.05). Data are represented as mean ± SEM. White bars represent control-fed mice and black bars represent MR-fed mice.

Figure 6. Body weight, composition, and serum insulin levels of male mice on long-term (190 days) MR diet (n = 7) compared to control diet (n = 8). (A) Body weight measurements taken over 190 days on MR diet or control diet. (B) Lean mass (g), (C) lean mass as a percentage of total body mass, (D) fat mass (g), and (E) fat mass as a percentage of total body mass were measured using NMR in mice fed MR diet or control diet. (F) Fasted serum insulin levels (ng/ml) measured following 190 days of MR diet or control diet. Significance was calculated by repeated measures two-way ANOVA with Bonferroni multiple comparison post hoc tests or 2-tailed Student's *t*-tests. Data are represented as mean ± SEM. White circles/bars represent control-fed mice and black circles/bars represent MR-fed mice.

Figure 7. Representative images of H and E stains obtained for kidney sections from a mouse that had been on long-term (190 days) MR diet showing (A) large vacuoles in a proximal renal tubule with normal renal tubules surrounding the one affected tubule and (B) large vacuoles present in 2 proximal tubules. (C) Bar chart showing scores, representing the number of tubule intersections containing vacuoles, obtained for individual mice within each treatment group. Correlation between the number of tubule intersections containing vacuoles and (D) body weight and (E) insulin levels for each individual mouse.

References

1. Huffman DM, Barzilai N. Role of visceral adipose tissue in aging. Biochim Biophys Acta. 2009 Oct;1790(10):1117-23.

2. Selman C, Withers DJ. Mammalian models of extended healthy lifespan. Philos Trans R Soc Lond B Biol Sci. 2011 Jan 12;366(1561):99-107.

3. Muzumdar R, Allison DB, Huffman DM, Ma X, Atzmon G, Einstein FH, et al. Visceral adipose tissue modulates mammalian longevity. Aging Cell. 2008 Jun;7(3):438-40.

4. Barzilai N, She L, Liu L, Wang J, Hu M, Vuguin P, et al. Decreased visceral adiposity accounts for leptin effect on hepatic but not peripheral insulin action. Am J Physiol. 1999 Aug;277(2 Pt 1):E291-8.

5. Orentreich N, Matias JR, DeFelice A, Zimmerman JA. Low methionine ingestion by rats extends life span. J Nutr. 1993 Feb;123(2):269-74.

6. Richie JP,Jr, Leutzinger Y, Parthasarathy S, Malloy V, Orentreich N, Zimmerman JA. Methionine restriction increases blood glutathione and longevity in F344 rats. FASEB J. 1994 Dec;8(15):1302-7.

7. Lees EK, Krol E, Grant L, Shearer K, Wyse C, Moncur E, et al. Methionine restriction restores a younger metabolic phenotype in adult mice with alterations in fibroblast growth factor 21. Aging Cell. 2014 Oct;13(5):817-27.

8. Zhou XJ, Rakheja D, Yu X, Saxena R, Vaziri ND, Silva FG. The aging kidney. Kidney Int. 2008 Sep;74(6):710-20.

9. Bitzer M, Wiggins J. Aging Biology in the Kidney. Adv Chronic Kidney Dis. 2016 Jan;23(1):12-8.

10. Weinstein JR, Anderson S. The aging kidney: physiological changes. Adv Chronic Kidney Dis. 2010 Jul;17(4):302-7.

11. Agouni A, Owen C, Czopek A, Mody N, Delibegovic M. In vivo differential effects of fasting, re-feeding, insulin and insulin stimulation time course on insulin signaling pathway components in peripheral tissues. Biochem Biophys Res Commun. 2010 Oct 8;401(1):104-11.

12. Pfaffl MW. A new mathematical model for relative quantification in real-time RT-PCR. Nucleic Acids Res. 2001 May 1;29(9):e45.

13. Saltiel AR, Kahn CR. Insulin signalling and the regulation of glucose and lipid metabolism. Nature. 2001 Dec 13;414(6865):799-806.

14. von Manteuffel SR, Dennis PB, Pullen N, Gingras AC, Sonenberg N, Thomas G. The insulin-induced signalling pathway leading to S6 and initiation factor 4E binding protein 1 phosphorylation bifurcates at a rapamycin-sensitive point immediately upstream of p70s6k. Mol Cell Biol. 1997 Sep;17(9):5426-36.

15. Strable MS, Ntambi JM. Genetic control of de novo lipogenesis: role in diet-induced obesity. Crit Rev Biochem Mol Biol. 2010 Jun;45(3):199-214.

16. Kim HW, Lee JE, Cha JJ, Hyun YY, Kim JE, Lee MH, et al. Fibroblast growth factor 21 improves insulin resistance and ameliorates renal injury in db/db mice. Endocrinology. 2013 Sep;154(9):3366-76.

17. Hu MC, Kuro-o M, Moe OW. Renal and extrarenal actions of Klotho. Semin Nephrol. 2013 Mar;33(2):118-29.

18. Kitada M, Kume S, Takeda-Watanabe A, Kanasaki K, Koya D. Sirtuins and renal diseases: relationship with aging and diabetic nephropathy. Clin Sci (Lond). 2013 Feb;124(3):153-64.

19. Hasek BE, Stewart LK, Henagan TM, Boudreau A, Lenard NR, Black C, et al. Dietary methionine restriction enhances metabolic flexibility and increases uncoupled respiration in both fed and fasted states. Am J Physiol Regul Integr Comp Physiol. 2010 Sep;299(3):R728-39.

20. Martin JE, Sheaff MT. Renal ageing. J Pathol. 2007 Jan;211(2):198-205.

21. Rodwell GE, Sonu R, Zahn JM, Lund J, Wilhelmy J, Wang L, et al. A transcriptional profile of aging in the human kidney. PLoS Biol. 2004 Dec;2(12):e427.

22. Plaisance EP, Henagan TM, Echlin H, Boudreau A, Hill KL, Lenard NR, et al. Role of beta-adrenergic receptors in the hyperphagic and hypermetabolic responses to dietary methionine restriction. Am J Physiol Regul Integr Comp Physiol. 2010 Sep;299(3):R740-50.

23. Ables GP, Perrone CE, Orentreich D, Orentreich N. Methionine-restricted C57BL/6J mice are resistant to diet-induced obesity and insulin resistance but have low bone density. PLoS One. 2012;7(12):e51357.

24. Baylis C, Corman B. The aging kidney: insights from experimental studies. J Am Soc Nephrol. 1998 Apr;9(4):699-709.

25. Hasek BE, Boudreau A, Shin J, Feng D, Hulver M, Van NT, et al. Remodeling the integration of lipid metabolism between liver and adipose tissue by dietary methionine restriction in rats. Diabetes. 2013 Oct;62(10):3362-72.

26. Patil YN, Dille KN, Burk DH, Cortez CC, Gettys TW. Cellular and molecular remodeling of inguinal adipose tissue mitochondria by dietary methionine restriction. J Nutr Biochem. 2015 Jul 22.

27. Friederich M, Nordquist L, Olerud J, Johansson M, Hansell P, Palm F. Identification and distribution of uncoupling protein isoforms in the normal and diabetic rat kidney. Adv Exp Med Biol. 2009;645:205-12.

28. Thomas J, Sweeney D, Liu J, Breen L, Printz M. Kidney-associated brown adipose tissue. Potential relationship to etiology of genetic hypertension in the SHR (spontaneously hypertensive rat). FASEB J. 2008;22 (Meeting Abstract Supplement):969.36.

29. Baylis C. Sexual dimorphism, the aging kidney, and involvement of nitric oxide deficiency. Semin Nephrol. 2009 Nov;29(6):569-78.

30. Black MJ, Lim K, Zimanyi MA, Sampson AK, Bubb KJ, Flower RL, et al. Accelerated age-related decline in renal and vascular function in female rats following early-life growth restriction. Am J Physiol Regul Integr Comp Physiol. 2015 Nov 1;309(9):R1153-61.

31. Zhang Y, Xie Y, Berglund ED, Coate KC, He TT, Katafuchi T, et al. The starvation hormone, fibroblast growth factor-21, extends lifespan in mice. Elife. 2012 Oct 15;1:e00065.

32. Cheng Y, Zhang J, Guo W, Li F, Sun W, Chen J, et al. Up-regulation of Nrf2 is involved in FGF21-mediated fenofibrate protection against type 1 diabetic nephropathy. Free Radic Biol Med. 2016 Apr;93:94-109.

33. Hu MC, Kuro-o M, Moe OW. Klotho and kidney disease. J Nephrol. 2010 Nov-Dec;23 Suppl 16:S136-44.

34. Zheng F, Plati AR, Potier M, Schulman Y, Berho M, Banerjee A, et al. Resistance to glomerulosclerosis in B6 mice disappears after menopause. Am J Pathol. 2003 Apr;162(4):1339-48.

35. Kitada M, Ogura Y, Suzuki T, Sen S, Lee SM, Kanasaki K, Kume S, Koya D. A very-low-protein diet ameliorates advanced diabetic nephropathy through autophagy induction by suppression of the mTORC1 pathway in Wistar fatty rats, an animal model of type 2 diabetes and obesity. Diabetologia. 2016 Jun;59(6):1307-17. doi: 10.1007/s00125-016-3925-4. Epub 2016 Mar 28.

Acknowledgements

This work was supported by the NHS Grampian project grant to MD, HMW and PAB, and Tenovus Scotland project grant to MD and NM. MD is funded by Diabetes UK and British Heart Foundation; NM was funded by the British Heart Foundation Intermediate Fellowship. EKL was funded by the BBSRC-DTG postgraduate studentship. This work was supported in part by the National Institutes of Health (RO1 DK-096311 to TWG).

Supplementary Material

Primer sequences

ACC1 F	GATGAACCATCTCCGTTGGC
ACC1 R	GACCCAATTATGAATCGGAGTG

ACC2 F	CGCTCACCAACAGTAAGGTGG
ACC2 R	GCTTGGCAGGGAGTTCCTC
Arginase F	CAGAAGAATGGAAGAGTCAG
Arginase R	CAGATATGCAGGGAGTCACC
β-actin F	GATCTGGCACCACACACCTTC
β-actin R	GGGGTGTTGAAGGTCTCAAA
CD11b F	CCCCACACTAGCATCAAGG
CD11b R	GAGGCAAGGGACACACTGA
CD68 F	TGTCTGATCTTGCTAGGACCA
CD68 R	GAGAGTAACGGCCTTTTTGTGA
F4/80 F	CCCAGCTTATGCCACCTGCA
F4/80 R	GTCCAGGCCCTGGAACATTGG
FAS F	GGAGGTGGTGATAGCCGGTAT
FAS R	TGGGTAATCCATAGAGCCCAG
G6Pase F	ATGAACATTCTCCATGACTTTGGG
G6Pase R	GACAGGGAACTGCTTTATTATAGG
GAPDH F	TGACCACAGTCCATGCCATC
GAPDH R	GACGGACACATTGGGGGTA
HPRT F	GTTAAGCAGTACAGCCCCAAA
HPRT R	AGGGCATATCCAACAACAAACTT
IL1 beta F	GCAACTGTTCCTGAACTCAACT
IL1 beta R	ATCTTTTGGGGTCCGTCAACT

IL4 F	GGTCTCAACCCCCAGCTAGT
IL4 R	GCCGATGATCTCTCTCAAGTGAT
IL4RA F	TCTGCATCCCGTTGTTTTGC
IL4RA R	GCACCTGTGCATCCTGAATG
IL6 F	TAGTCCTTCCTACCCCAATTTCC
IL6 R	TTGGTCCTTAGCCACTCCTTC
IL10 F	GCTCTTACTGACTGGCATGAG
IL10 R	CGCAGCTCTAGGAGCATGTG
Klotho F	GGGACACTTTCACCCATCACT
Klotho R	ACGTTGTTGTAACTATCGCTGG
βKlotho F	TGTTCTGCTGCGAGCTGTTAC
βKlotho R	CCGGACTCACGTACTGTTTTT
MCP-1 F	TTAAAAACCTGGATCGGAACCAA
MCP-1 R	GCATTAGCTTCAGATTTACGGGT
NoNo F	GCCAGAATGAAGGCTTGACTAT
NoNo R	TATCAGGGGGAAGATTGCCCA
PDGF-B F	CATCCGCTCCTTTGATGATCTT
PDGF-B R	GTGCTCGGGTCATGTTCAAGT
PEPCK F	GAGATAGCGGCACAAT
PEPCK R	TTCAGAGACTATGCGGTG
PGC1α F	AACCACACCCACAGGATCAGA
PGC1α R	TCTTCGCTTTATTGCTCCATGA

PPARγ F	AGTGGAGACCGCCCAGG
PPARγ R	GTAGCAGGTTGTCTTGAATGT
SCD1 F	TTCTTGCGATACACTCTGGTGC
SCD1 R	CGGGATTGAATGTTCTTGTCGT
Sirt1 F	TGATTGGCACAGATCCTCG
Sirt1 R	CCACAGTGTCATATCATCCAA
SREBP1 F	ATGTGCGAACTGGACACAGCG
SREBP1 R	AGGCTGTAGGATGGTGAGTGG
SREBP2 F	CCCTTGACTTCCTTGCTGCA
SREBP2 R	GCGTGAGTGTGGGCGAATC
TFAM F	ATTCCGAAGTGTTTTTCCAGCA
TFAM R	TCTGAAAGTTTTGCATCTGGGT
TGFβ F	AGCCCGAAGCGGACTACTAT
TGFβ R	CTGTGTGAGATGTCTTTGGTTTTC
TNF-alpha F	CCCTCACACTCAGATCATCTTCT
TNF-alpha R	GCTACGACGTGGGCTACAG
UCP1 F	AGGCTTCCAGTACCATTAGGT
UCP1 R	CTGAGTGAGGCAAAGCTGATTT
UCP2 F	ATGGTTGGTTTCAAGGCCACA
UCP2 R	CGGTATCCAGAGGGAAAGTGAT
YWhaz F	GAAAAGTTCTTGATCCCCAATGC
YWhaz R	TGTGACTGGTCCACAATTCCTT

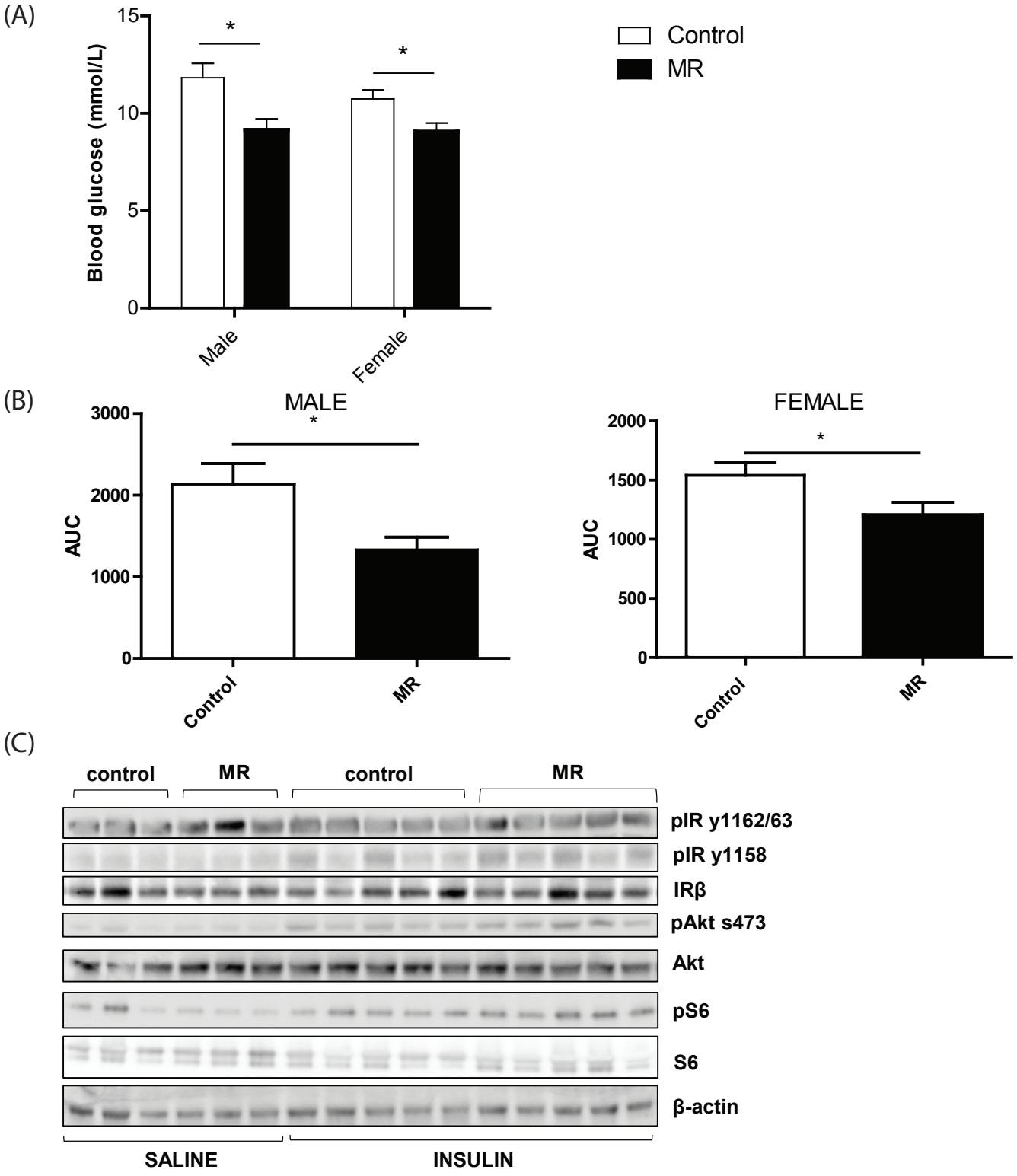
(A)
Blood glucose (mmol/L)
15
10
5
0
*
*
Male
Female
Control
MR
(B)
MALE
FEMALE
AUC
3000
2000
1000
0
2000
1500
1000
500
*
*
Control
MR
(C)
control
MR
control
MR
pIR y1162/63
pIR y1158
IRβ
pAkt s473
Akt
pS6
S6
β-actin
SALINE
INSULIN
(D)
Fold change
2.0
1.5
1.0
0.5
0.0
CON saline
CON insulin
MR saline
MR insulin
p-IR y1162/63
p-IR y1158
p-Akt
p-S6

Figure 1

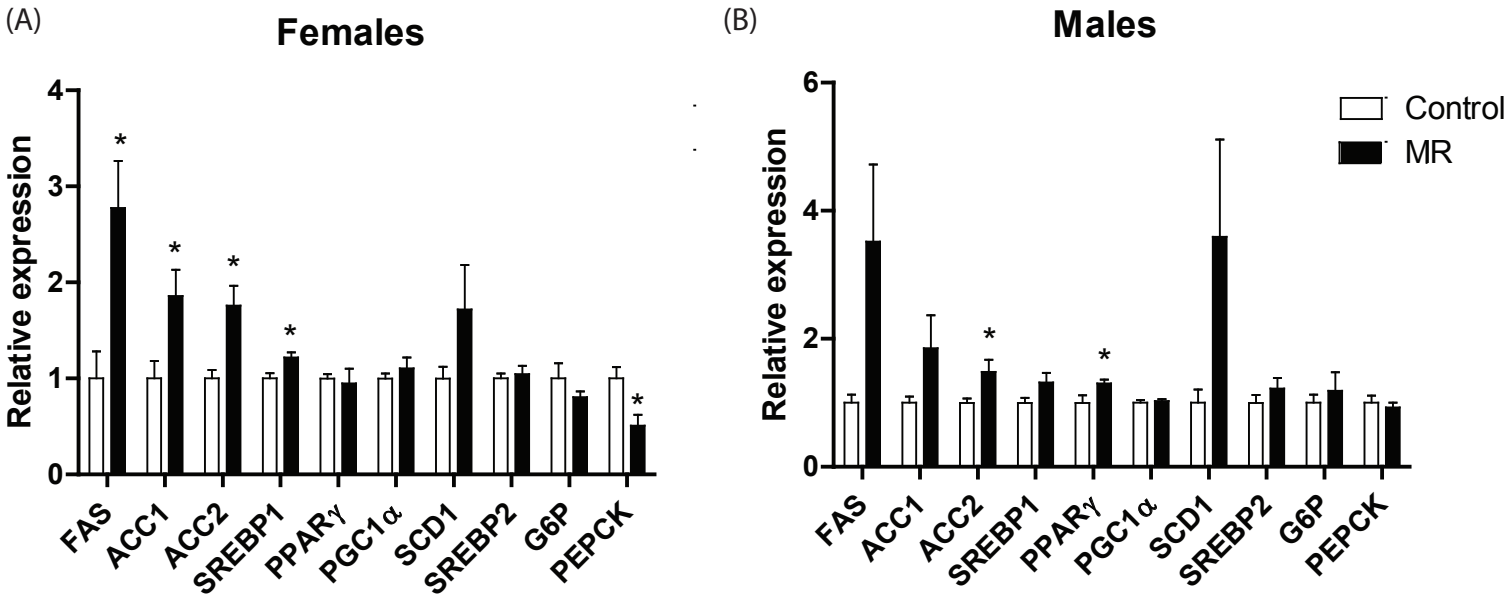
(A)
Females
Relative expression
0
1
2
3
4
*
*
*
*
*
FAS
ACC1
ACC2
SREBP1
PPARγ
PGC1α
SCD1
SREBP2
G6P
PEPCK
(B)
Males
Relative expression
0
2
4
6
*
*
Control
MR
FAS
ACC1
ACC2
SREBP1
PPARγ
PGC1α
SCD1
SREBP2
G6P
PEPCK

Figure 2

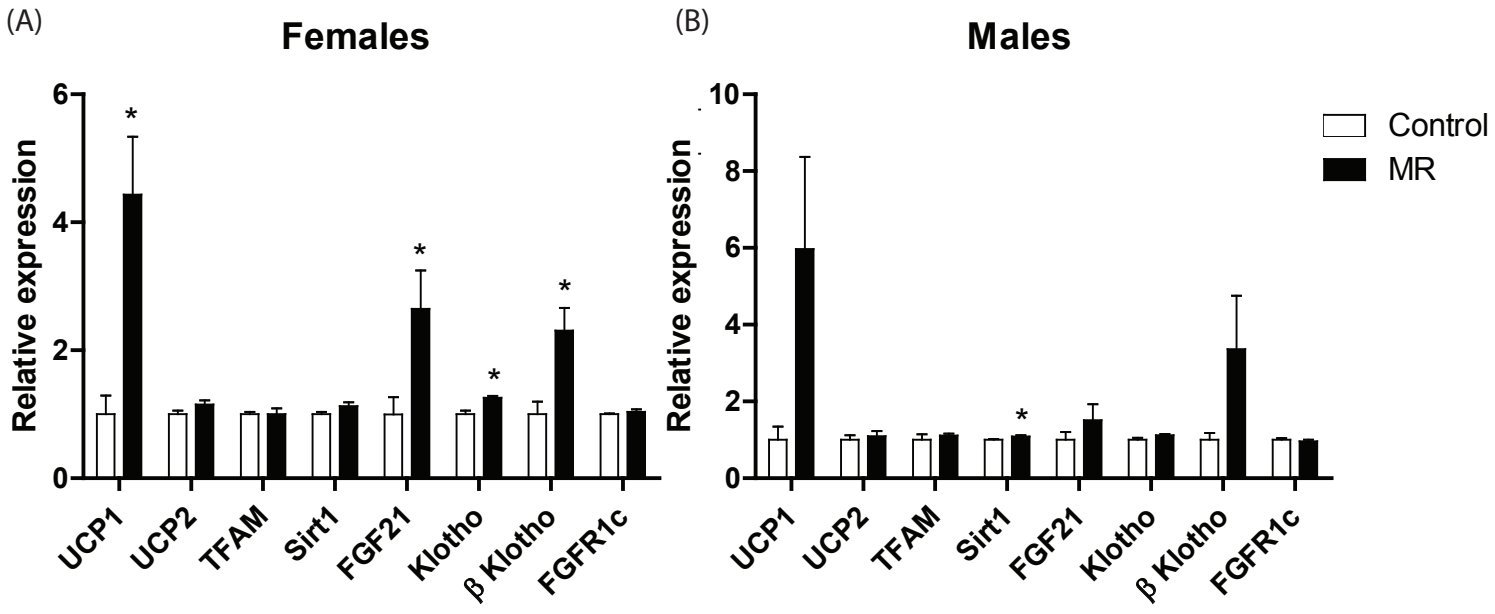
(A)
Females
Relative expression
6
4
2
0
*
*
*
UCP1
UCP2
TFAM
Sirt1
FGF21
Klotho
β Klotho
FGFR1c
(B)
Males
Relative expression
10
8
6
4
2
0
*
UCP1
UCP2
TFAM
Sirt1
FGF21
Klotho
β Klotho
FGFR1c
Control
MR

Figure 3

(A)

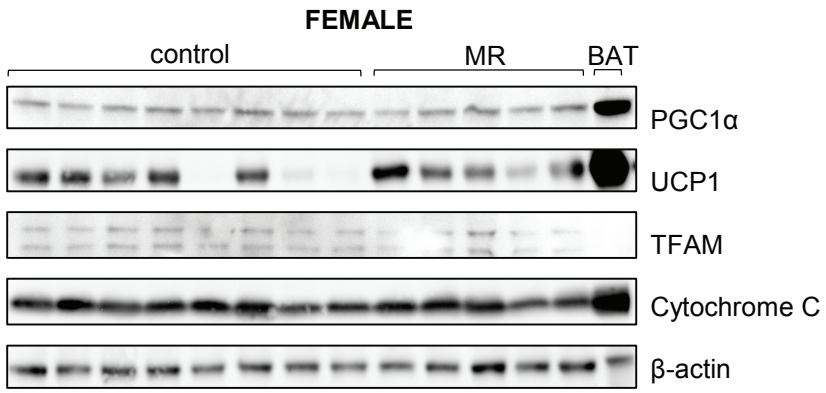
FEMALE
control
MR
BAT
PGC1α
UCP1
TFAM
Cytochrome C
β-actin

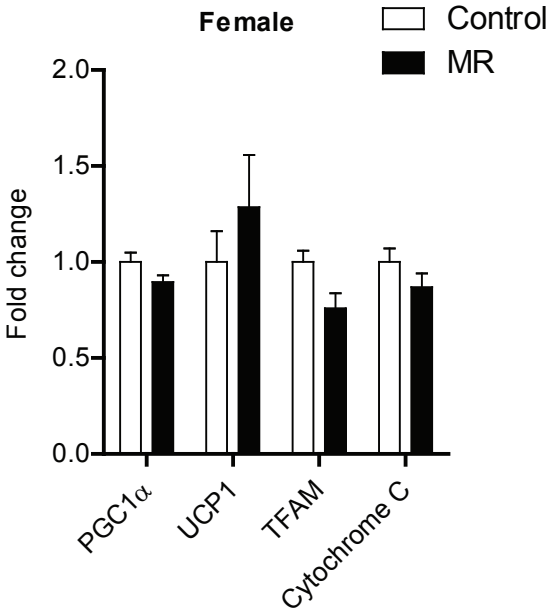
Female
Control
MR
Fold change
2.0
1.5
1.0
0.5
0.0
PGC1α
UCP1
TFAM
Cytochrome C

(B)

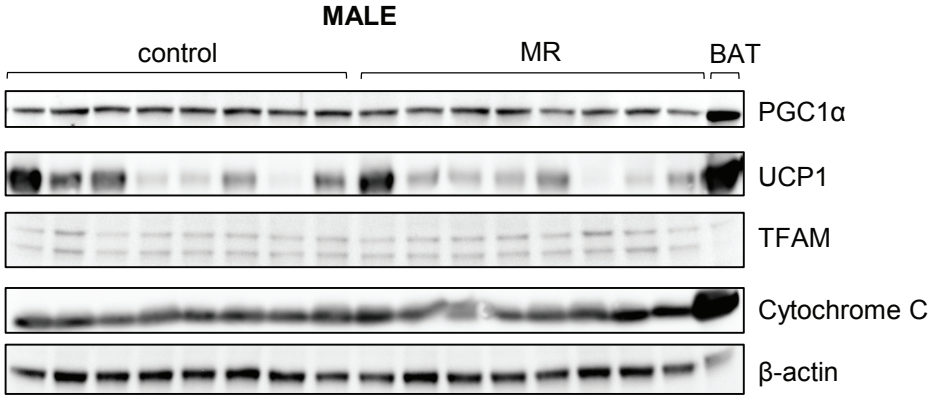
MALE
control
MR
BAT
PGC1α
UCP1
TFAM
Cytochrome C
β-actin

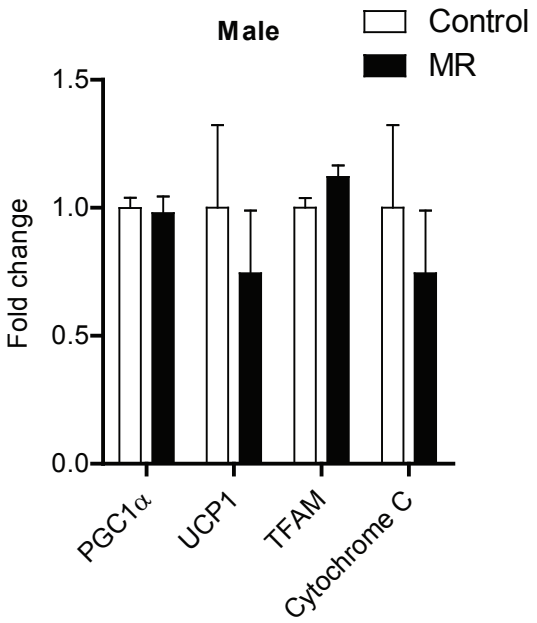
Male
Control
MR
Fold change
1.5
1.0
0.5
0.0
PGC1α
UCP1
TFAM
Cytochrome C

Figure 4

(A)

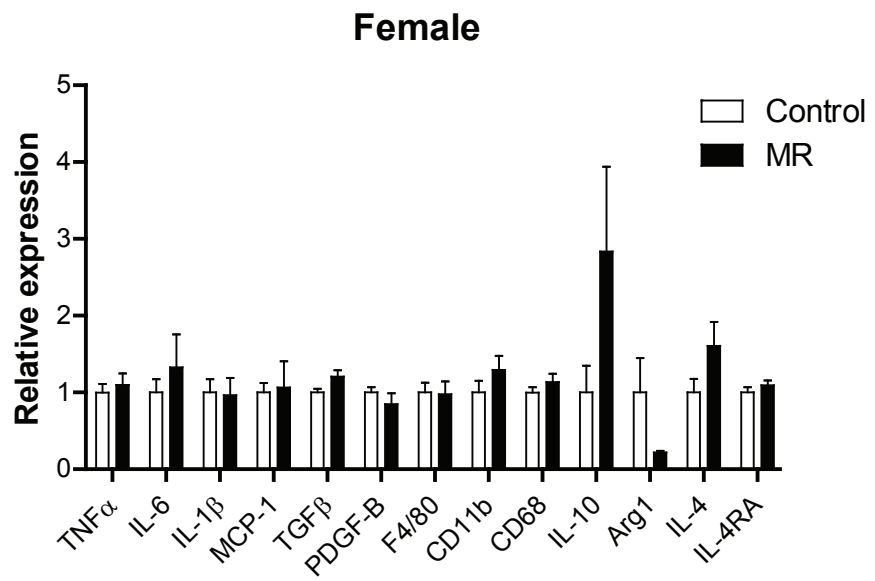
Female
Relative expression
Control
MR
0
1
2
3
4
5
TNFα
IL-6
IL-1β
MCP-1
TGFβ
PDGF-B
F4/80
CD11b
CD68
IL-10
Arg1
IL-4
IL-4RA

(B)

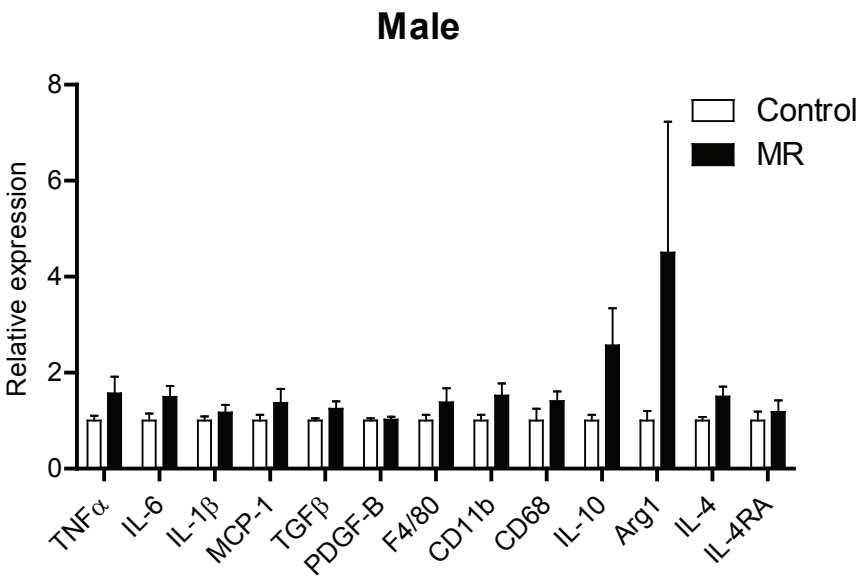
Male
Relative expression
Control
MR
0
2
4
6
8
TNFα
IL-6
IL-1β
MCP-1
TGFβ
PDGF-B
F4/80
CD11b
CD68
IL-10
Arg1
IL-4
IL-4RA

Figure 5

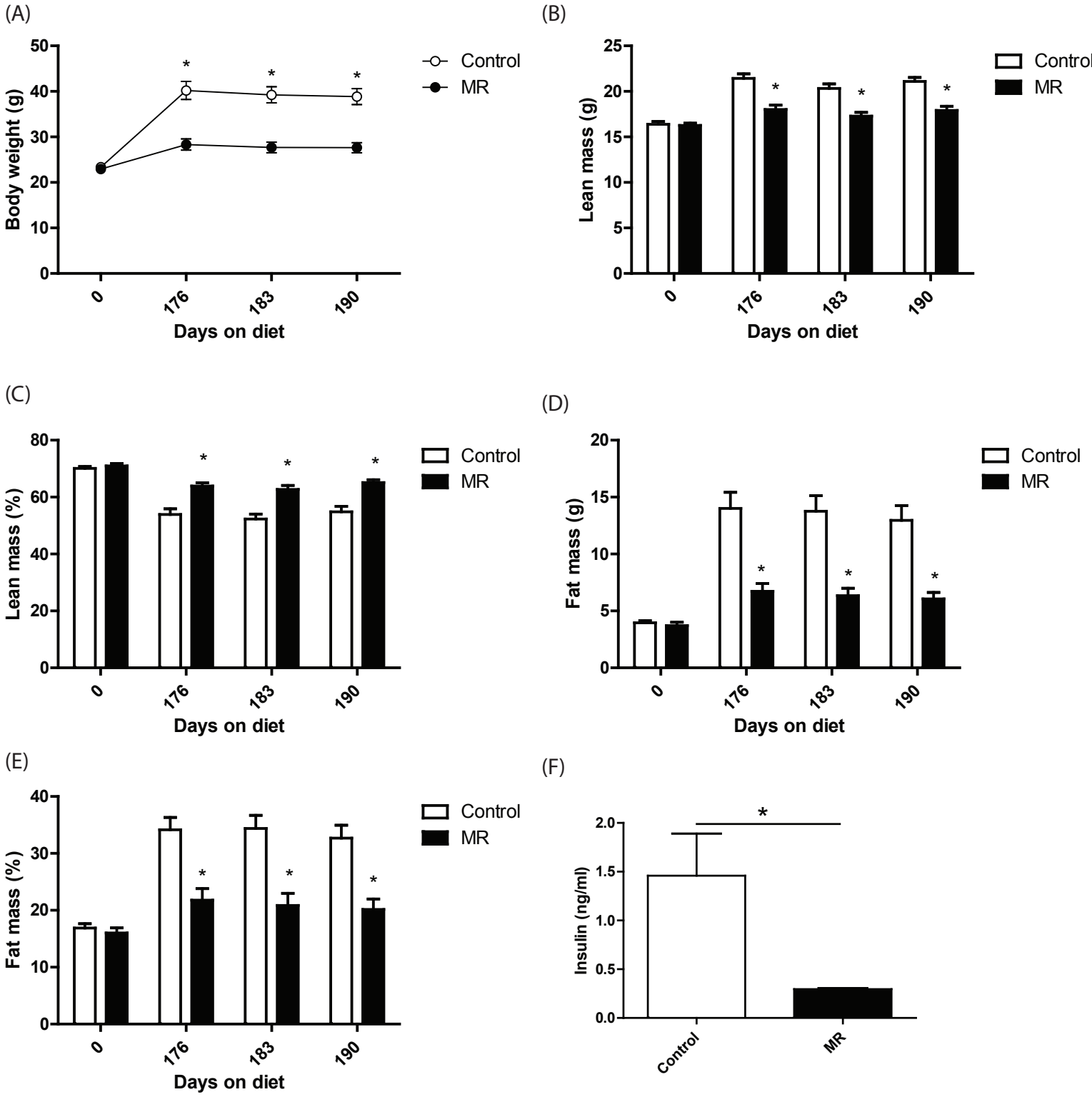
(A)
Body weight (g)
Control
MR
Days on diet
(B)
Lean mass (g)
Control
MR
Days on diet
(C)
Lean mass (%)
Control
MR
Days on diet
(D)
Fat mass (g)
Control
MR
Days on diet
(E)
Fat mass (%)
Control
MR
Days on diet
(F)
Insulin (ng/ml)
Control
MR

Figure 6